2000

Self-Discharge Model of a Nickel-Hydrogen Cell

B. Wu

Ralph E. White
University of South Carolina - Columbia, white@cec.sc.edu

Publication Info

Published in *Journal of the Electrochemical Society*, Volume 147, Issue 3, 2000, pages 902-909.

Wu, B., & White, R.E. (2000) Self-Discharge Model of a Nickel-Hydrogen Cell. *Journal of the Electrochemical Society*, *147*(3) 902-909.
Publisher's Version: http://dx.doi.org/10.1149/1.1393290

Journal of The Electrochemical Society, **147** (3) 902-909 (2000)
S0013-4651(99)08-010-6 CCC: $7.00

Self-Discharge Model of a Nickel-Hydrogen Cell

B. Wu and R. E. White*,z

Center for Electrochemical Engineering, Department of Chemical Engineering, University of South Carolina, Columbia, South Carolina 29208, USA

A model of the self-discharge process of a nickel-hydrogen cell is presented. The model includes three electrochemical reactions on the nickel electrode (reduction of nickel oxyhydroxide, oxidation of hydrogen, and oxidation of hydroxyl ion to form oxygen) and two electrochemical reactions on the hydrogen electrode (reduction of oxygen and oxidation of hydrogen). The self-discharge pressure profile of the nickel-hydrogen battery that consists of two characteristic regions is explained reasonably well with the model. The model can be used to predict the capacity retention of a nickel-hydrogen cell during open-circuit conditions at different temperatures.

Manuscript submitted August 4, 1999; revised manuscript received November 4, 1999.

The nickel-hydrogen battery is well known for its high energy density, good overcharge tolerance, and long cycle life, and has been the primary energy storing system for aerospace applications during the last two decades. Unfortunately, the nickel-hydrogen battery shows a relatively high self-discharge rate compared to other batteries (including other nickel-based batteries). It is important to determine the self-discharge rate (the capacity retention) of a nickel-hydrogen battery during open-circuit stand prior to launch and during the transfer orbit period in the aerospace applications.[1]

The self-discharge process of the nickel electrode alone and the whole nickel-hydrogen cell have been investigated by some researchers.[2-6] Stockel[2] used a logarithm expression to fit the measured capacity retention of a nickel-hydrogen cell at different temperatures, which showed significant influences of temperature on the self-discharge process. Conway and Bourgault[3] investigated the kinetics of oxygen evolution during the self-discharge of the nickel electrode and proposed that the observed potential of the nickel electrode is a mixed potential of both nickel reaction and oxygen reaction. Kim *et al.*[4] summarized several different forms of approximate equations for the self-discharge pressure profile of a nickel-hydrogen cell and proposed that the hydrogen oxidation is a direct chemical reaction by measuring the heat generation rate of a nickel electrode in the hydrogen environment. Mao and White[5] developed a mathematical model of a flooded nickel electrode in the hydrogen environment to explain qualitatively the self-discharge behavior by assuming chemical reaction between the hydrogen and the nickel electrode. Through constant-potential experiments, Mao and White[6] showed that hydrogen oxidation on the nickel electrode is an electrochemical reaction and estimated the rate and order of that reaction. Leblanc *et al.*[7] identified three paths of self-discharge in a nickel-metal hydride battery (different from the nickel-hydrogen battery in the negative electrode) and showed that some redox shuttles in the electrolyte may exist and increase the self-discharge rate of the nickel metal hydride battery. Experimental data have shown that there are two characteristic regions in the pressure curve (fast pressure drop in the first region and slow pressure drop in the second region) during self-discharge of a nickel-hydrogen cell, which have not been explained satisfactorily by previous researchers. In this work, a mathematical model that can reasonably explain the self-discharge behavior of a nickel-hydrogen cell is proposed. The following self-discharge mechanism is used: (*i*) electrochemical oxidation of hydrogen on the nickel electrode, and (*ii*) evolution of oxygen on the nickel electrode and then reduction of oxygen on the hydrogen electrode (with simultaneous hydrogen oxidation).[1,7] The comparison of the model predictions to experimental data and some simulation results are presented and analyzed.

* Electrochemical Society Fellow.
z E-mail: white@engr.sc.edu

Self-Discharge Modeling of a Nickel-Hydrogen Cell

In a typical nickel-hydrogen cell, there are tens of modules in the cell stack (see Fig. 1). Each module consists of four components: nickel electrode, separator, hydrogen (platinum) electrode, and gas screen. It is generally accepted that there are five electrochemical reactions occurring on the porous nickel and hydrogen electrodes[1,8] as shown below (Eq. 1-5)

Nickel electrode

$$NiOOH + H_2O + e^- \underset{\text{charge}}{\overset{\text{discharge}}{\rightleftharpoons}} Ni(OH)_2 + OH^- \qquad [1]$$

$$2\ OH^- \rightarrow \frac{1}{2} O_2 + H_2O + 2e^- \qquad [2]$$

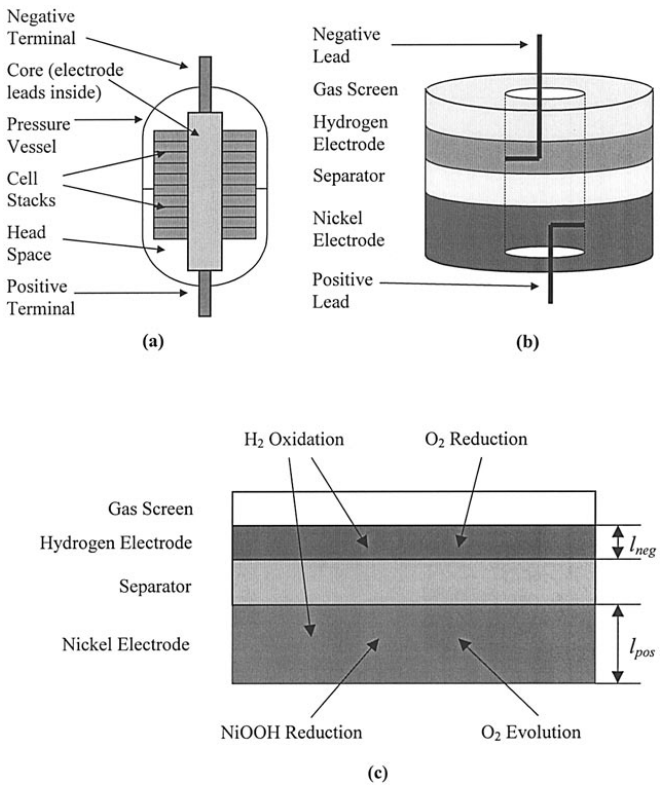

Figure 1. Schematic diagrams of (a) a nickel-hydrogen cell, (b) one module of the cell stack, and (c) self-discharge reactions in a nickel-hydrogen cell module.

S0013-4651(99)08-010-6 CCC: $7.00

$$\frac{1}{2}H_2 + OH^- \rightarrow H_2O + e^- \quad [3]$$

Hydrogen electrode

$$\frac{1}{2}H_2 + OH^- \underset{\text{charge}}{\overset{\text{discharge}}{\rightleftharpoons}} H_2O + e^- \quad [4]$$

$$\frac{1}{2}O_2 + H_2O + 2e^- \rightarrow 2\ OH^- \quad [5]$$

Arrows used in Eq. 2, 3, and 4 indicate unidirectional reactions due to favorable overpotentials for these reactions. It is generally believed that hydrogen reactions Eq. 3 and 4 are one-electron-transfer reactions and oxygen reactions Eq. 2 and Eq. 5 are two-electron-transfer reactions. The redox reactions of nickel active materials are much more complex than those described by Eq. 1,[9-12] and may involve several different phases and reactions with perhaps more than one electron transfers. However, for simplicity, it is assumed that the nickel reaction is a one-electron-transfer reaction in the form of Eq. 1. During open-circuit stand (self-discharge process), there is no current across the separator, and self-discharge reactions occur on both positive (nickel) and negative (hydrogen) electrodes as shown in Fig. 1. The following charge balance relations exist

$$j_1 + j_2 + j_3 = 0 \quad [6]$$

$$j_4 + j_5 = 0 \quad [7]$$

On the nickel electrode, nickel oxyhydroxide is reduced while oxygen is evolved and hydrogen is oxidized, and the absolute value of the rate of reaction Eq. 1 is equal to that of the sum of the rates of reactions Eq. 2 and 3. On the hydrogen electrode, oxygen is reduced while hydrogen is oxidized, and the absolute value of the rate of reaction Eq. 4 is equal to that of reaction Eq. 5. There is a gas diffusion path that links the self-discharge processes on the positive electrode to those on the negative electrodes: oxygen evolved on the nickel electrodes will diffuse to the hydrogen electrodes and be reduced there. Compared to the kinetics of the self-discharge reactions, the gas diffusion process is very rapid, and uniform gas concentration in a nickel-hydrogen cell can be assumed. The cell stack of a nickel-hydrogen cell is not flooded with electrolyte. During the activation stage of a nickel-hydrogen cell, some electrolyte in the cell stack was pushed out by gas evolution and then drained out. Thus some gas volume exists in the cell stack, which provides a gas diffusion path in the cell stack.[1] Consequently, in the model presented here, the reactions are assumed to occur uniformly throughout the electrode (*i.e.*, the current densities do not depend on location inside the electrode).

Since there is no chemical limitation of hydrogen generation from electrolyte (excess water in electrolyte) and the hydrogen reaction on the platinum is highly reversible, the nickel electrode is the capacity-limiting electrode in a nickel-hydrogen cell, and the property of the nickel electrode has significant influence on the cell behavior. One important feature of the nickel electrode is its hysteresis potential behavior,[9,10] *i.e.*, the charge-discharge potential curve of the nickel electrode forms a hysteresis loop where the potential of the discharge process is always lower than that of the charge process despite the charge and discharge rates. The value of the difference ranges from 70 to 110 mV for different types of nickel electrodes.[9] The detailed chemical and physical processes involved in the hysteresis process is still unknown. In this work, an empirical approach is used (see Fig. 2): the charge and discharge potentials of a nickel electrode are represented differently.

For the charge process, the open-circuit potential for the nickel electrode is given by

$$\phi_{eq,1,T} = U^{\theta}_{1,c} - U^{\theta}_{RE} + (T - T_0)\left(\frac{dU_1}{dT} - \frac{dU_{RE}}{dT}\right) + \frac{RT}{F}\ln\left(\frac{x}{1-x}\right) \quad [8]$$

For the discharge process, a simple modification of Eq. 8 with negative offset gives

$$\phi_{eq,1,T} = U^{\theta}_{1,c} - U^{\theta}_{RE} + (T - T_0)\left(\frac{dU_1}{dT} - \frac{dU_{RE}}{dT}\right) + \frac{RT}{F}\ln\left(\frac{x}{1-x}\right) - (U^{\theta}_{1,c} - U^{\theta}_{1,d}) \quad [9]$$

However, Eq. 9 showed significant error at high state of charge (SOC) region. Adding an empirical term to Eq. 9 yields the apparent open-circuit potential expression for the nickel electrode for the discharge process

$$\phi_{eq,1,T} = U^{\theta}_{1,c} - U^{\theta}_{RE} + (T - T_0)\left(\frac{dU_1}{dT} - \frac{dU_{RE}}{dT}\right) + \frac{RT}{F}\ln\left(\frac{x}{1-x}\right) - (U^{\theta}_{1,c} - U^{\theta}_{1,d}) + (U^{\theta}_{1,c} - U^{\theta}_{1,d})\exp[-k_1(1-x)] \quad [10]$$

In the above equations, the Hg/HgO electrode has been used as the reference electrode, and the temperature variation of open-circuit potentials has also been included. In the last term of Eq. 10, k_1 is a parameter that influences the potential dropping in the early discharge stage. It has negligible influence on the potential at medium and low SOC levels. The fitting of the charge/discharge potential curves of a nickel film electrode[9] with Eq. 8, 9, and 10 is shown in Fig. 2. The improvement over Eq. 9 at high SOC of the discharge potential curve is obvious with the empirical term in Eq. 10. Since there are kinetic overpotentials involved in the experimental data from Ref. 9, the fitting in Fig. 2 is only a rough approximation. Accurate determination of nickel equilibrium potential curve needs more rigorous experiment and analysis.[3]

The potential of a nickel electrode has displayed little sensitivity to the change of current densities. The rate of the redox reaction of the nickel active materials is normally believed to be very rapid. A Tafel coefficient as small as 10 mV/dec has been observed when ohmic effects are carefully eliminated.[9] Moreover, the reaction rates of self-discharge are normally very small; the overpotential that drives the reduction of nickel species can then be neglected. Hence, during self-discharge, the potential of the nickel electrode can be treated as staying at the apparent open-circuit potential of nickel active materials (in the form of Eq. 10).

The oxygen evolution reaction is very sluggish on the nickel electrode, which is clearly indicated by the overcharge potential plateau during the normal operations of the nickel-hydrogen battery. During self-discharge, the driving force for this reaction is the high potential

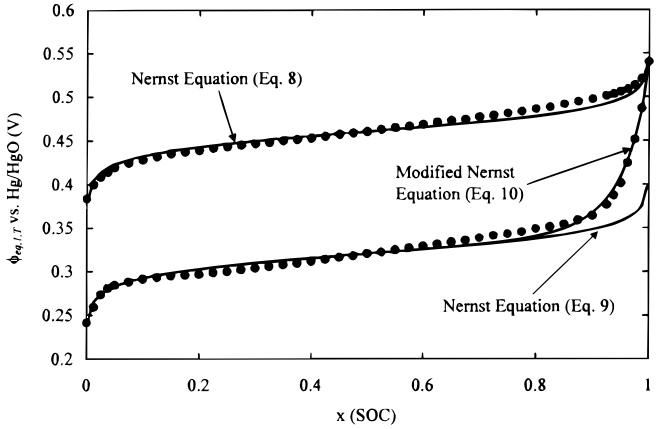

Figure 2. The hysteresis potential behavior of the nickel electrode. The dot points are experimental data from Ref. 9.

S0013-4651(99)08-010-6 CCC: $7.00

of the oxidized nickel active species. The reaction rate of the oxygen evolution can be expressed in a Butler-Volmer equation form

$$j_2 = j_{o,2,ref,T}\left[\left(\frac{c_e}{c_{e,ref}}\right)^2 \exp\left(\frac{\alpha_{a2}F}{RT}\eta_2\right) - \left(\frac{p_{O_2}}{p_{O_2,ref}}\right)^{\frac{1}{2}} \exp\left(-\frac{\alpha_{c2}F}{RT}\eta_2\right)\right] \quad [11]$$

Similar to the derivation for the overpotential of the oxygen reduction reaction on the hydrogen (platinum) electrode in the Appendix, the overpotential for the oxygen evolution reaction on the nickel electrode can be expressed as

$$\eta_2 = \phi_{eq,1,T} - \phi_{eq,2,ref,T} \quad [12]$$

where $\phi_{eq,2,ref,T}$ is the equilibrium potential of oxygen evolution reaction at a reference condition, which can be calculated from the Nernst equation

$$\phi_{eq,2,ref,T} = U_2^\theta - U_{RE}^\theta + (T - T_0)\left(\frac{dU_2}{dT} - \frac{dU_{RE}}{dT}\right) + \frac{RT}{2F}\ln(p_{O_2,ref})^{\frac{1}{2}} \quad [13]$$

Similar to the oxygen evolution reaction, the reaction rate of hydrogen oxidation on the nickel electrode is given by

$$j_3 = j_{o,3,ref,T}\left[\left(\frac{c_e}{c_{e,ref}}\right)\left(\frac{p_{H_2}}{p_{H_2,ref}}\right)^{\frac{1}{2}} \exp\left(\frac{\alpha_{a3}F}{RT}\eta_3\right) - \exp\left(-\frac{\alpha_{c3}F}{RT}\eta_3\right)\right] \quad [14]$$

with

$$\eta_3 = \phi_{eq,1,T} - \phi_{eq,3,ref,T} \quad [15]$$

The equilibrium potential of this reaction at a reference condition is expressed by

$$\phi_{eq,3,ref,T} = U_3^\theta - U_{RE}^\theta + (T - T_0)\left(\frac{dU_3}{dT} - \frac{dU_{RE}}{dT}\right) - \frac{RT}{F}\ln(p_{H_2,ref})^{\frac{1}{2}} \quad [16]$$

The exchange current densities in Eq. 11 and 14 are temperature dependent and can be written in an Arrhenius equation form

$$j_{0,k,ref,T} = j_{0,k,ref,T_0} \exp\left[-\frac{\Delta E_k}{R}\left(\frac{1}{T} - \frac{1}{T_0}\right)\right] \quad \text{for} \quad k = 2, 3 \quad [17]$$

Since the electrochemical driving force is very high for oxygen reduction on the hydrogen electrode as shown in the Appendix, a limiting current form for oxygen reduction is used[13]

$$j_5 = -j_{5,ref,T_0}\left(\frac{p_{O_2}}{p_{O_2,ref}}\right)\exp\left[-\frac{\Delta E_5}{R}\left(\frac{1}{T} - \frac{1}{T_0}\right)\right] \quad [18]$$

where the activation energy is for the oxygen diffusion process in the electrolyte.

Due to the rapid oxygen reduction reaction on the hydrogen electrode, the oxygen concentration in a nickel-hydrogen cell is always very low. Even during *C* rate overcharge, oxygen accounts for only a small fraction of the gas phase.[1] Since water vapor is also in negligible amount at normal temperatures, the gas phase in a nickel-hydrogen cell can be treated as consisting of hydrogen only. Then the capacity of a nickel-hydrogen cell can be easily correlated to the cell pressure, a fact that has been widely used in industry to estimate the cell capacity. In fact, from the charge balance of a nickel-hydrogen cell, a simple expression between the SOC of the nickel electrode and the hydrogen amount in the cell can be obtained

$$x = \frac{n_{H_2} - n_{H_2,init}}{n_{H_2,full} - n_{H_2,init}} \quad [19]$$

The above expression is valid for both negative (hydrogen) precharge and positive precharge nickel-hydrogen cells. The positive precharge needs to be converted to the equivalent amount of hydrogen expressed by a negative value. With the ideal-gas law

$$n_{H_2} = \frac{p_{H_2}V_{gas}}{RT} \quad [20]$$

the amount of hydrogen gas can be expressed in cell pressure. Substitution of Eq. 20 into Eq. 19 yields

$$x = \frac{p_{H_2} - p_{H_2,init,T}}{p_{H_2,full,T} - p_{H_2,init,T}} \quad [21]$$

The initial and full cell pressure in Eq. 21 will be different at different temperatures, and they can be expressed with respect to a reference temperature using the ideal-gas law

$$p_{H_2,init,T} = \frac{Tp_{H_2,init,T_0}}{T_0} \quad [22]$$

$$p_{H_2,full,T} = \frac{Tp_{H_2,full,T}}{T_0} \quad [23]$$

With Eq. 21, the discharge potential of the nickel electrode Eq. 10 can be expressed as

$$\phi_{eq,1,T} = U_{1,c}^\phi - U_{RE}^\theta + (T - T_0)\left(\frac{dU_1}{dT} - \frac{dU_{RE}}{dT}\right) + \frac{RT}{F}\ln\left(\frac{p_{H_2} - p_{H_2,init,T}}{p_{H_2,full,T} - p_{H_2}}\right) - (U_{1,c}^\theta - U_{1,d}^\theta)\left[1 - \exp\left(-k_1\frac{p_{H_2,full,T} - p_{H_2}}{p_{H_2,full,T} - p_{H_2,init,T}}\right)\right] \quad [24]$$

It has long been observed that the capacity (hence the hydrogen pressure when fully charged) of a nickel-hydrogen cell will vary with many factors, such as charging scheme, temperature, KOH concentration, etc. The accurate prediction of the capacity of a nickel-hydrogen cell at different conditions is very difficult due to the complex mechanisms inside the nickel-hydrogen cell. Thus it is more feasible that the fully charged hydrogen pressure $p_{H_2,full,T}$ be taken directly from the experimental measurements. The empirical parameter k_1 corresponding to $p_{H_2,full,T}$ also needs to be fitted from a potential curve measured at a low discharge rate, *e.g.*, C/5. The normal charging scheme for a nickel-hydrogen cell is the C/10 rate for 16 h at 10°C in experiments. The pressure at the end of this process can be used as $p_{H_2,full,T}$ to obtain $p_{H_2,full,T_0}$.

Due to the electrochemical reactions, the amount of hydrogen and oxygen in a nickel-hydrogen cell will change. Since there are negligible amounts of dissolved hydrogen and oxygen, the mass balances of hydrogen and oxygen in a nickel-hydrogen cell can be expressed by

$$\frac{V_{gas}}{RT}\frac{dp_{H_2}}{dt} = \frac{1}{2F}N_m A_e(a_{pos}l_{pos}j_3 + a_{neg}l_{neg}j_4) \quad [25]$$

$$\frac{V_{gas}}{RT}\frac{dp_{O_2}}{dt} = \frac{1}{4F}N_m A_e(a_{pos}l_{pos}j_2 + a_{neg}l_{neg}j_5) \quad [26]$$

S0013-4651(99)08-010-6 CCC: $7.00

With the charge balance of Eq. 7, Eq. 25 can be rewritten as

$$\frac{V_{gas}}{RT}\frac{dp_{H_2}}{dt} = \frac{1}{2F}N_m A_e(a_{pos}l_{pos}j_3 - a_{neg}l_{neg}j_5) \quad [27]$$

The combination of Eq. 11-18, 24, 26, and 27 constitutes the model for the self-discharge process of a nickel-hydrogen cell and the model can be used to predict hydrogen pressure, oxygen pressure, potential of the nickel electrode, and relevant reaction rates during the self-discharge process. The popular public-domain differential and algebraic equation (DAE) solver DASSL[14] has been used in this work to solve the above model equations.

Results and Discussion

The parameters used in the model are listed in Table I. One important parameter, the gas volume inside a nickel-hydrogen cell can be estimated from experimental data. The experimental data of INTELSAT VIIA cell (120 Ah rated capacity) during self-discharge are used to validate the model predictions.[1] The INTELSAT VIIA cell is charged at C/10 for 16 h at 10°C, then stays on open circuit for 6 days at three different temperatures 10, 20, and 30°C. The logarithmic relationship that has been used in industry is[1,2]

$$\ln(C_{pct}) = \ln(C_{pct,0}) - k_2 t \quad [28]$$

where the percent capacity remaining C_{pct} is expressed by cell pressure

$$C_{pct} = \frac{P_{cell}}{P_{cell,0}} \quad [29]$$

and $C_{pct,0}$ is a fitted value that is usually not equal to 100 (as it should be) due to the limitation of the expression. The fitting of the pressure curves with Eq. 28 to experimental data yields the following equations[1,2]

$$\ln(C_{pct}) = \ln(86.487) - 0.00104\frac{t}{3600} \qquad T = 10°C \quad [30]$$

$$\ln(C_{pct}) = \ln(88.293) - 0.00191\frac{t}{3600} \qquad T = 20°C \quad [31]$$

$$\ln(C_{pct}) = \ln(89.999) - 0.00329\frac{t}{3600} \qquad T = 30°C \quad [32]$$

The unit conversion from second to hour has been explicitly included in the above equations to be consistent in parameters with Ref. 1 and 2. The corresponding pressure curves are shown in Fig. 3. It is clear that the logarithmic fitting is good for the second stage of self-discharge, but is not valid for the early stage of the self-discharge, which can cause the artifact of different $C_{pct,0}$ values.

The model's predictions of the cell-pressure profile ($P_{cell} = p_{H_2} + p_{O_2}$) for the INTELSAT VIIA nickel-hydrogen cell during 6 days' self-discharge compared to the experimental data are shown in Fig. 4. Two regions of different characteristics in the cell pressure curve are both satisfactorily matched. The corresponding potentials of the nickel electrode are shown in Fig. 5. Comparison of the two figures indicates that there is some shape similarity between the cell pressure curves and the potential curves of the nickel electrode. The difference between the potentials at different temperatures in Fig. 5 is partly due to the negative temperature coefficient of the nickel reaction. Another cause of the potential difference is that the SOC of the nickel electrode at the same time point at different temperatures is not the same due to different self-discharge rates, *i.e.*, SOC drops faster at high temperatures.

The total current of each self-discharge reaction at 20°C is shown in Fig. 6, which provides an obvious clue about the two characteristic regions of the cell pressure curve that cannot be fitted well for the whole range by other mechanisms. The self-discharge rate of the

Table I. Parameter values used in the simulation.

Parameter	Value	Source[a]
N_m	48	Ref. 13[b]
A_e	100 cm^2	Ref. 13[b]
a_{pos}	4000 cm^2/cm^3	Ref. 13[b]
l_{pos}	0.072 cm	Ref. 13[b]
a_{neg}	1250 cm^2/cm^3	Ref. 13[b]
l_{neg}	0.02 cm	Ref. 13[b]
V_{gas}	1044.3 cm^3	
c_e	5.8×10^{-3} mol/cm^3	
$c_{e,ref}$	5.8×10^{-3} mol/cm^3	
$j_{o,2,ref,T_0}$	8×10^{-10} A/cm^2	
$j_{o,3,ref,T_0}$	5×10^{-18} A/cm^2	
j_{5,ref,T_0}	5×10^{-3} A/cm^2	
k_1	15	
$p_{H_2,ref}$	1 atm	
$p_{O_2,ref}$	1 atm	
$p_{H_2,init,T_0}$	−5.0 atm	
$p_{H_2,full,T_0}$	53.8 atm	
T_0	298.15 K	
U^{θ}_{RE}	0.0983 V	Ref. 16
$U^{\theta}_{l,c}$	0.527 V	
$U^{\theta}_{l,d}$	0.427 V	
U^{θ}_2	0.4011 V	Ref. 16
U^{θ}_3	−0.8280 V	Ref. 16
U^{θ}_4	−0.8280 V	Ref. 16
dU_{RE}/dt	−1.125 mV/K	Ref. 16
dU_1/dT	−1.35 mV/K	Ref. 16
dU_2/dT	−1.6816 mV/K	Ref. 16
dU_3/dT	−0.836 mV/K	Ref. 16
dU_4/dT	−0.836 mV/K	Ref. 16
α_{a2}	1.25	Ref. 8
α_{c2}	0.75	Ref. 8
α_{a3}	0.5	Ref. 8
α_{c3}	0.5	Ref. 8
ΔE_2	100 kJ/K	
ΔE_3	120 kJ/K	
ΔE_5	15 kJ/K	
Initial conditions		
p_{H_2} (T = 10°C)	51.1 atm	
p_{H_2} (T = 20°C)	52.9 atm	
p_{H_2} (T = 30°C)	54.7 atm	
p_{O_2} (T = 10°C)	1×10^{-4} atm	
p_{O_2} (T = 20°C)	1×10^{-4} atm	
p_{O_2} (T = 30°C)	1×10^{-4} atm	

[a] The parameters that have no source listed are either assumed values or design parameters.
[b] Estimated from the TRW 30 Ah cell in Ref. 13.

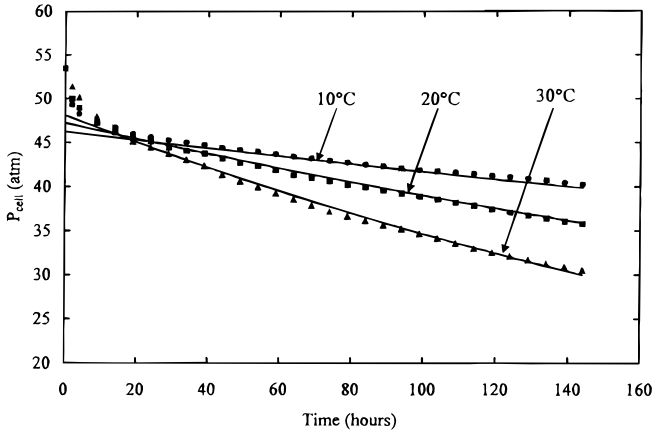

Figure 3. The fitting results of the logarithm expression for the pressure profile during self-discharge of the INTELSAT VIIA cell (data points from Ref. 1).

S0013-4651(99)08-010-6 CCC: $7.00

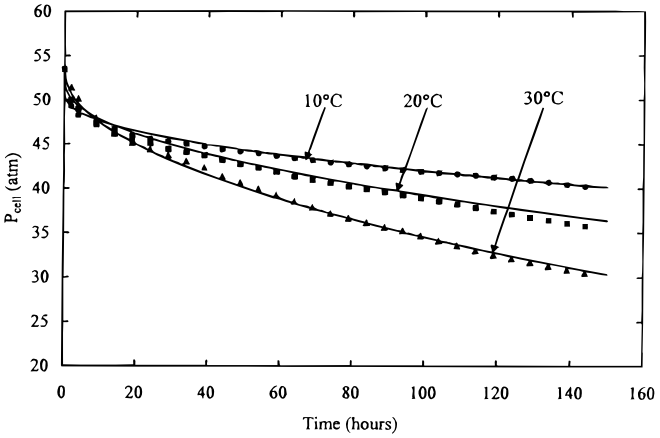

Figure 4. Model predicted cell-pressure profile compared to the experimental data of the INTELSAT VIIA cell (data points from Ref. 1).

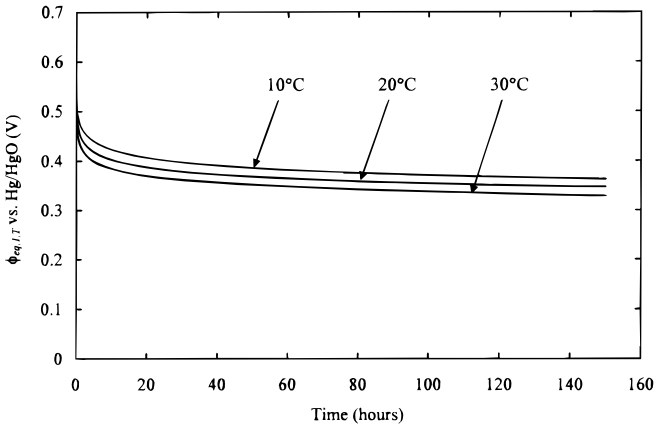

Figure 5. Model predicted nickel electrode potential profile at different temperatures.

nickel-hydrogen cell can be as high as 1.2 A (C/100) at the early stage of the self-discharge, but it is only about 0.25 A (C/500) after the early stage of the self-discharge. The two characteristic regions of the self-discharge process are caused by the potential behavior of the nickel electrode at different SOCs as summarized in Fig. 7. The high potential of the nickel electrode at the early stage of the self-discharge (high SOCs) causes high rates of oxygen evolution and hydrogen oxidation that in turn causes the fast pressure drop (fast capacity loss)

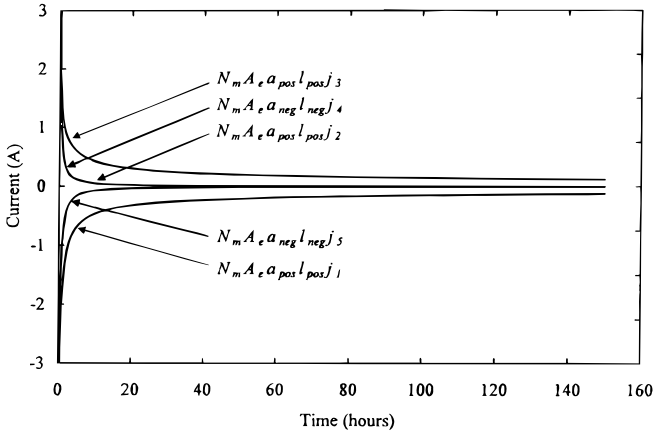

Figure 6. Model predicted total current of each self-discharge reaction at 20°C.

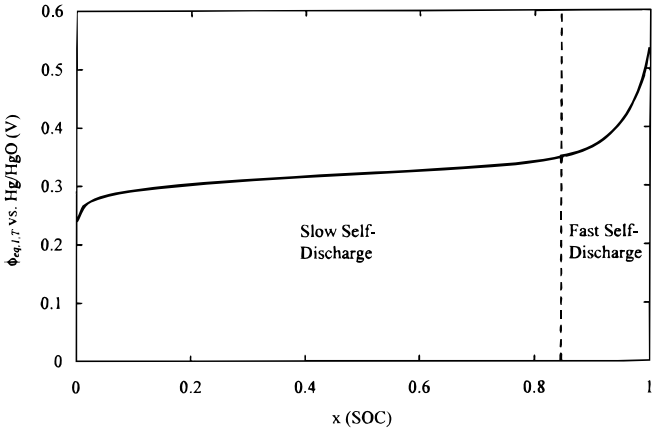

Figure 7. Two characteristic regions during the self-discharge process of a nickel-hydrogen cell caused by the potential behavior of the nickel electrode.

during the early stage of the self-discharge. After the first stage of the self-discharge, the relatively low potential of the nickel electrode remains to be fairly constant as explained by the Nernst equation for medium SOCs. Thus the driving forces for the self-discharge reactions Eq. 11 and 14 remain almost constant. A comparatively slow pressure drop process (slow capacity loss) then dominates, and an approximate logarithmic cell pressure profile is obtained.

It is also observed from Fig. 6 that the current of oxygen reduction on the hydrogen electrode is almost equal to that of the oxygen evolution on the nickel electrode, which implies that there is no oxygen accumulation in the nickel-hydrogen cell. In fact, the oxygen partial pressure during the self-discharge process at 20°C is shown in Fig. 8. The oxygen pressure remains very low and is at least four orders of magnitude smaller than that of hydrogen. Thus the assumption that the cell pressure in the nickel-hydrogen cell can be approximated by hydrogen pressure during self-discharge is reasonable.

The current densities of oxygen evolution and hydrogen oxidation on the nickel electrode at three temperatures are shown in Fig. 9 and 10, respectively. It is observed that the rate of oxygen evolution is comparable to that of hydrogen oxidation for the first several hours. Afterward, it is much smaller than that of the hydrogen oxidation. Thus the hydrogen oxidation is shown to be the main path of the self-discharge process in a nickel-hydrogen cell, which confirms the experimental result obtained by Mao and White.[6]

It is observed in Fig. 4 that the self-discharge rate is much faster at high temperatures than at low temperatures. The reason is that both the oxygen evolution rate and hydrogen oxidation rate increase with temperatures as shown in the predicted current densities in Fig. 9 and

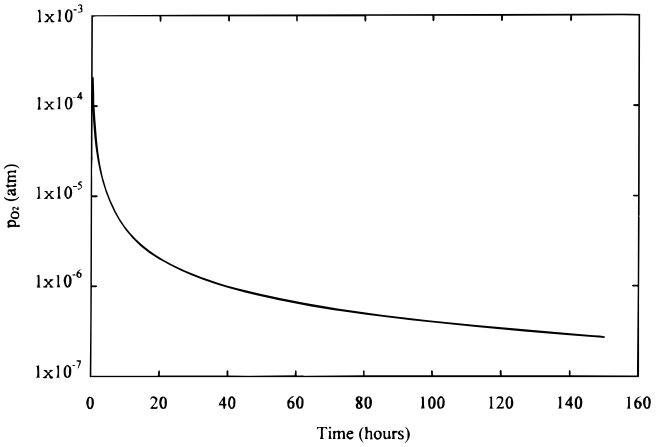

Figure 8. Model predicted oxygen partial pressure profile at 20°C.

S0013-4651(99)08-010-6 CCC: $7.00

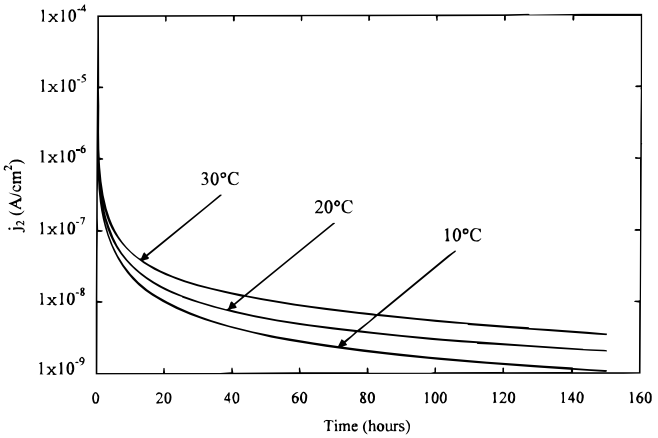

Figure 9. Model predicted current density of oxygen evolution on the nickel electrode at different temperatures.

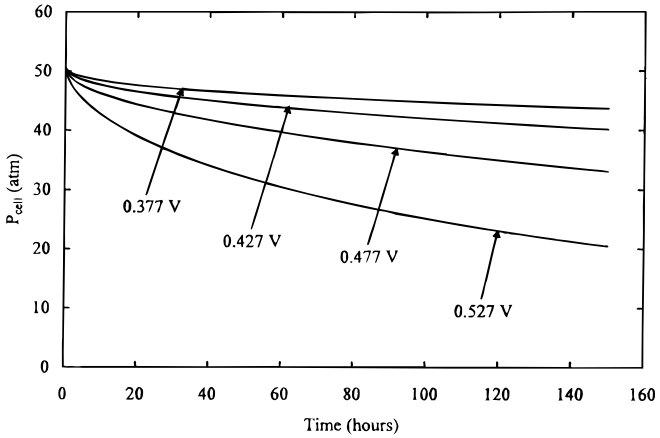

Figure 11. Model predicted cell-pressure profile for different apparent open-circuit potentials of the nickel reaction at 10°C.

10. These two reactions are sensitive to temperature changes as indicated by the high values of their activation energies.

In Fig. 11, the simulated cell-pressure profiles with different apparent open-circuit potentials of the nickel electrode are shown. It is interesting to notice that if the open-circuit potential of the nickel reaction during the discharge process remains the same as that of the charge process, *i.e.*, with no hysteresis effect, the self-discharge of a nickel-hydrogen cell will be a faster process. This is because the high potential of the nickel active materials can cause faster oxygen evolution and hydrogen oxidation reactions. However, self-discharge with that fast rate is not observed in the real life. Hence, the hysteresis potential behavior, *i.e.*, separation of the charge and discharge potential of the nickel electrode, actually makes possible the storage of the nickel-hydrogen cells for a medium time length, *i.e.*, several days. The significant influence of potential hysteresis on the self-discharge also points out that, when modeling the behavior of the nickel electrode, reversible charge/discharge potential behavior cannot be assumed. A more accurate (and probably more complex) model of the charge/discharge reactions must be used, or an empirical correction for the difference between the charge/discharge potential behavior as presented above must be made; otherwise, significant error will be obtained.

Great sensitivity of the self-discharge rate with respect to the apparent value of open-circuit potential of the nickel reaction during the self-discharge process is also observed in Fig. 11. Even an increase of 50 mV of the apparent open-circuit potential of the nickel reaction will cause the self-discharge rate to be doubled. The reason is the exponential relation of the reaction rates of the oxygen evolution and hydrogen oxidation reactions with respect to the nickel electrode potential. Any factors that influence the open-circuit potential of the nickel electrode, such as the cycling process, electrolyte concentration, or chemical additives to the nickel active materials or electrolyte, will affect the self-discharge rate of the nickel-hydrogen cell.

As can be inferred from Eq. 11 and 12, increasing the equilibrium potential of oxygen evolution on the nickel electrode (*e.g.*, by using chemical additives in nickel active materials or electrolyte) can be a valid approach to reduce the self-discharge rate of the nickel-hydrogen cell by reducing the oxygen evolution rate. But the main self-discharge process, hydrogen oxidation on the nickel electrode, must be hindered to achieve more effective reduction of the self-discharge rate. Some additives to the nickel active materials, such as cobalt hydroxide and cadmium hydroxide, which have been used to increase charge acceptance during the charge process, can both decrease the open-circuit potential of the nickel reaction and increase the apparent equilibrium potential of the oxygen reaction. They will have the beneficial effects of decreasing the self-discharge rate of the nickel-hydrogen cell by decreasing the rates of both oxygen and hydrogen reactions on the nickel electrode.

The self-discharge by the path of oxygen evolution only is shown in Fig. 12. It is observed that the self-discharge rate is much less than that with both oxygen evolution and hydrogen oxidation reactions. In fact, the self-discharge rate in this case is similar to that of the nickel-cadimum battery. Thus, it is reasonable to conclude that the high self-discharge rate of a nickel-hydrogen battery compared to other nickel-based batteries is due to the electrochemical oxidation

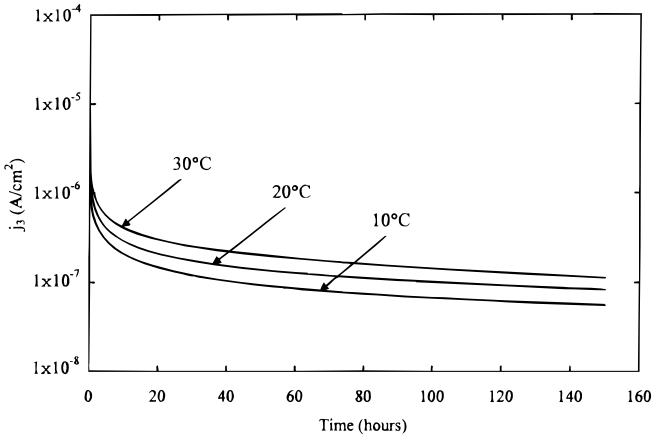

Figure 10. Model predicted current density of hydrogen oxidation on the nickel electrode at different temperatures.

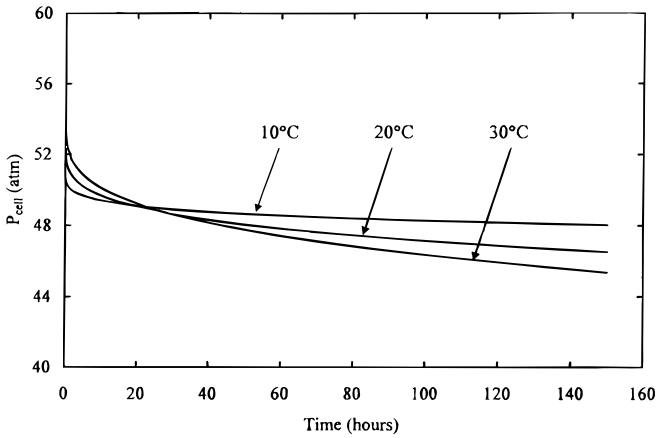

Figure 12. Model predicted cell pressure profile at different temperatures with the self-discharge path of oxygen evolution only.

S0013-4651(99)08-010-6 CCC: $7.00

of the hydrogen on the nickel-electrode. Then, the most effective approach to reduce the self-discharge of the nickel-hydrogen cell is to reduce the hydrogen oxidation process on the nickel electrode. Using a flooded nickel electrode can reduce the effective reaction area for hydrogen oxidation on the nickel-electrode due to the diffusion limitation of dissolved hydrogen and would therefore slow down the self-discharge rate of the nickel electrode.[5] However, because the explosive reaction of oxygen and hydrogen gas can cause structural damage to the nickel-hydrogen cell stack, using a flooded cell is not a feasible approach to reduce the self-discharge of a nickel-hydrogen cell. Then hindrance of the hydrogen reaction rate by chemical additives would be a preferred approach to reduce the self-discharge of a nickel-hydrogen cell.

Conclusions

A model of the self-discharge process of a nickel-hydrogen cell has been presented. It is shown that satisfactory predictions of the self-discharge process of a nickel-hydrogen cell can be obtained by considering two primary self-discharge paths: (*i*) hydrogen oxidation on the nickel electrode and (*ii*) oxygen evolution on the nickel electrode and then reduction on the platinum electrode (with simultaneous hydrogen oxidation). The main reason for the high discharge rate of the nickel-hydrogen battery compared to other nickel-based batteries is shown to be hydrogen oxidation on the nickel electrode. It is proposed that self-discharge of nickel-hydrogen cells can be reduced by lowering the open-circuit potential of the nickel-active materials, and reducing the hydrogen oxidation rate on the nickel electrode.

Acknowledgments

The authors gratefully acknowledge the financial support from the Office of Research and Development of the United States Central Intelligence Agency.

The University of South Carolina assisted in meeting the publication costs of this article.

Appendix

Mass-Transfer Limitation of Oxygen Reduction on the Platinum Electrode

For simplicity, only the reaction rate at 25°C is calculated here. The electrochemical reaction rate of the oxygen reduction on the platinum electrode can be expressed by a Bulter-Volmer equation in the form

$$j_5 = j_{o,5,ref,T_0}\left[\left(\frac{c_e}{c_{e,ref}}\right)^2 \exp\left(\frac{\alpha_{a5}F}{RT}\eta_5\right) - \left(\frac{p_{O_5}}{p_{O_2,ref}}\right)^{\frac{1}{2}} \exp\left(-\frac{\alpha_{c5}F}{RT}\eta_5\right)\right] \quad [A\text{-}1]$$

where the overpotential can be expressed as

$$\eta_5 = \phi_{neg} - \phi_{neg,l} - \phi_{eq,5,ref,T_0} \quad [A\text{-}2]$$

Since the hydrogen reaction on the platinum electrode is very rapid, the overpotential for reaction Eq. 4 can be treated as a small value

$$\eta_4 = \phi_{neg} - \phi_{neg,l} - \phi_{eq,4,T_0} \approx 0 \quad [A\text{-}3]$$

or

$$\phi_{neg} - \phi_{neg,l} \approx \phi_{eq,4,T_0} \quad [A\text{-}4]$$

Then we have

$$\eta_5 \approx \phi_{eq,4,T_0} - \phi_{eq,5,ref,T_0} \quad [A\text{-}5]$$

The equilibrium potential of reaction Eq. 4 can be calculated by

$$\phi_{eq,4,T_0} = U_4^\theta - U_{RE}^\theta - \frac{RT}{2F}\ln(p_{H_2}) \quad [A\text{-}6]$$

The equilibrium potential of the oxygen reduction at a reference condition is

$$\phi_{eq,5,ref,T_0} = U_5^\theta - U_{RE}^\theta + \frac{RT}{4F}\ln(p_{O_2,ref}) \quad [A\text{-}7]$$

Thus the overpotential for oxygen reduction can be expressed by

$$\eta_5 \approx U_4^\theta - U_5^\theta - \frac{RT}{4F}\ln(p_{H_2}^2 p_{O_2}) = -1.229 - \frac{RT}{4F}\ln(p_{H_2}^2 p_{O_2}) \quad [A\text{-}8]$$

Assuming an oxygen pressure of 0.01 atm, a hydrogen pressure of 10 atm, and KOH electrolyte of the reference concentration, we have

$$\eta_5 \approx -1.229 - \frac{RT}{4F}\ln(p_{H_2}^2 p_{O_2}) = -1.229 \text{ V} \quad [A\text{-}9]$$

For an exchange current density $j_{o,5,ref} = 10^{-10}$ A/cm^2, and the apparent transfer coefficients $\alpha_{a5} = 1.00$ and $\alpha_{c5} = 1.00$, [15] we have for Eq. A-1

$$j_5 = -10^{-10} \times \left[\exp\left(\frac{96487}{8.314 \times 298.15}[-1.229]\right) - (0.01)^{\frac{1}{2}} \exp\left(-\frac{96487}{8.314 \times 298.15}[-1.229]\right)\right] \approx -6.0 \times 10^{10} \text{ A/cm}^2 \quad [A\text{-}10]$$

Therefore, the mass-transfer limitation must exist for oxygen reduction on the platinum electrode, and Eq. A-1 cannot be used for the oxygen reduction on the platinum electrode.

List of Symbols

a_{pos}	specific surface area of the nickel electrode, cm^2/cm^3
a_{neg}	specific surface area of the hydrogen (platinum) electrode, cm^2/cm^3
A_e	projected electrode area of the cell module, cm^2
c_e	concentration of KOH electrolyte, mol/cm^3
$c_{e,ref}$	reference concentration of KOH electrolyte, mol/cm^3
C	capacity of a nickel-hydrogen cell, Ah
$C_{dis,0}$	initial capacity of a nickel-hydrogen cell before discharge, Ah
C_{pct}	percent of the initial capacity of a nickel-hydrogen cell
$C_{pct,0}$	parameter in logarithmic fitting of the capacity of a nickel-hydrogen cell
dU_k/dT	temperature coefficient of the equilibrium potential of reaction k, V/K
F	Faraday's constant, 96,487 C/equiv
j_k	local current density due to reaction k at the solid-liquid interface, A/cm^2
$j_{o,k,ref,T}$	exchange current density of reaction k at reference reactant concentrations and temperature T, A/cm^2
j_{5,ref,T_0}	reaction rate of oxygen reduction on the platinum electrode at reference oxygen pressure and temperature T, A/cm^2
k_1	constant in the expression of the discharge potential of a nickel electrode
k_2	constant in the expression of the logarithm fitting of the remaining capacity of a nickel-hydrogen cell during self-discharge, s^{-1}
l_{pos}	thickness of the nickel electrode, cm
l_{neg}	thickness of the hydrogen (platinum) electrode, cm
n_{H_2}	moles of hydrogen in a nickel-hydrogen cell, mol
$n_{H_2,init}$	moles of hydrogen in a nickel-hydrogen cell at fully discharged state, mol
$n_{H_2,full}$	moles of hydrogen in a nickel-hydrogen cell at fully charged state, mol
n_{O_2}	moles of oxygen in a nickel-hydrogen cell, mol
N_m	number of modules in a nickel-hydrogen cell
p_{H_2}	partial pressure of hydrogen, atm
$p_{H_2,ref}$	reference pressure of hydrogen, atm
$p_{H_2,init,T}$	precharged pressure of hydrogen at temperature T, atm
$p_{H_2,full,T}$	pressure of hydrogen at temperature T when cell is fully charged, atm
p_{O_2}	partial pressure of oxygen, atm
$p_{O_2,ref}$	reference pressure of oxygen, atm
P_{cell}	pressure of a nickel-hydrogen cell, atm
$P_{cell,0}$	initial pressure of a nickel-hydrogen cell before self-discharge, atm
$P_{dis,0}$	initial pressure of a nickel-hydrogen cell before discharge, atm
R	universal gas constant, 8.3143 J/mol/K or 82.0562 atm cm^3/mol/K
SOC	state of charge
t	time, s
T	temperature, K

S0013-4651(99)08-010-6 CCC: $7.00

T_0	reference temperature, 298.15 K
x	state of charge (SOC) of the nickel electrode
U_k^θ	standard equilibrium potential of reaction *k*, V
$U_{1,c}^\theta$	apparent standard open-circuit potential of the nickel active materials during the charge process, V
$U_{1,d}^\theta$	apparent standard open-circuit potential of the nickel active materials during the discharge process, V
V_{gas}	internal gas volume in a nickel-hydrogen cell, cm^3

Greek

α_{ak}	anodic transfer coefficient of reaction *k*
α_{ck}	cathodic transfer coefficient of reaction *k*
ΔE_k	activation energy of reaction *k*, kJ/mol
ϕ_{pos}	potential of the nickel active materials at the solid-liquid interface on the nickel electrode where the electrochemical reactions occur, V
$\phi_{pos,l}$	potential of the electrolyte phase at the solid-liquid interface on the nickel electrode where the electrochemical reactions occur, V
ϕ_{neg}	potential of the platinum black at the solid-liquid interface on the platinum electrode where the electrochemical reactions occur, V
$\phi_{neg,l}$	potential of the electrolyte phase at the solid-liquid interface on the platinum electrode where the electrochemical reactions occur, V
$\phi_{eq,k,T}$	equilibrium potential of reaction *k* at temperature *T*, V
$\phi_{eq,k,ref,T}$	equilibrium potential of reaction *k* at reference reactant concentrations and temperature *T*, V
η_k	overpotential of reaction *k*, V

References

1. J. D. Dunlop, G. M. Rao, and T. Y. Yi, *NASA Handbook for Nickel-Hydrogen Batteries*, NASA Reference Publication 1314 (1993).
2. J. F. Stockel, in *Proceedings of the 20th InterSociety Energy Conversion Engineering Conference*, p. 1171 (1985).
3. B. E. Conway and P. L. Bourgault, *Can J. Chem.*, **37,** 292 (1959).
4. Y. J. Kim, A. Visintin, S. Srinivasan, and A. J. Appleby, in *Nickel Hydroxide Electrodes*, D. A. Corrigan and A. H. Zimmerman, Editors, PV 90-4, p. 368, The Electrochemical Society Proceedings Series, Pennington, NJ (1990).
5. Z. Mao and R. E. White, *J. Electrochem. Soc.*, **138,** 3354 (1991).
6. Z. Mao and R. E. White, *J. Electrochem. Soc.*, **139,** 1282 (1992).
7. P. Leblanc, P. Blanchard, and S. Senyarich, *J. Electrochem. Soc.*, **145,** 844 (1998).
8. P. De Vidts, J. Delgado, and R. E. White, *J. Electrochem. Soc.*, **143,** 3223 (1996).
9. P. C. Milner and U. B. Thomas, in *Advances in Electrochemistry and Electrochemical Engineering*, Vol. 5, C. W. Tobias, Editor, p. 1, Interscience, New York (1967).
10. J. McBreen, in *Modern Aspects of Electrochemistry*, No. 21, R. E. White, J. O'M. Bockris, and B. E. Conway, Editors, p. 29, Plenum Press, New York (1990).
11. P. Oliva, J. Leonardi, J. F. Laurent, C. Delmas, J. J. Braconnier, M. Figlarz, F. Fievet, and A. de Guibert, *J. Power Sources*, **8,** 229 (1982).
12. G. Halpert, *J. Power Sources*, **12,** 177 (1984).
13. P. De Vidts, J. Delgado, B. Wu, D. See, K. Kosanovich, and R. E. White, *J. Electrochem. Soc.*, **145,** 3874 (1998).
14. K. E. Brenan, S. L. Campbell, and L. R. Petzold, *Numerical Solution of Initial-Value Problems in Differential-Algebraic Equations*, North-Holland, New York (1989).
15. S. Park, S. Ho, S. Aruliah, M. F. Weber, C. A. Ward, and R. D. Venter, *J. Electrochem. Soc.*, **133,** 1641 (1986).
16. S. G. Bratsch, *J. Phys. Chem. Ref. Data*, **18,** 1 (1989).